

STUDY ON THE APPLICABILITY OF CAST STEEL OVERPACK -EVALUATION OF CASTING DEFECTS AND CORROSION RESISTANCE USING FULL-SCALE PROTOTYPE-

Yusuke Ogawa, Satoru Suzuki, Kazuhisa Yamashina, Shigeru Kubota

Nuclear Waste Management Organization of Japan (NUMO)

2F, Mita NN Bldg, 4-1-23, Shiba, Minato-ku, Tokyo, Japan

Key words; Geological disposal, Overpack, Cast steel, Non-destructive test, Corrosion, Polarization tests

Abstract

The corrosion resistance of cast steel overpack, which may be effective to reduce manufacturing cost as compared with forged steel overpack, was examined. The specimens were taken from a cast steel overpack manufactured on a full-scale to reproduce realistic distributions of microstructure, chemical composition and casting defects. Consequently, there were only negligible heterogeneities of distributions of microstructure and chemical composition and no difference of corrosion behavior between specimens. On the other hand, the casting defects showed the heterogeneous distribution and concentrated to the lower half of overpack. These casting defects were distributed in the region including the corrosion allowance layer. Thus, the influences of these defects on the corrosion allowance and the treatment in the design of thickness of overpack were discussed.

1. Introduction

In Japanese geological disposal concept, high-level radioactive waste (HLW) is contained in a metal container, referred to as overpack. Overpack is required to have containment for at least 1,000 years, and the reference material is carbon steel [1].

Carbon steel materials are classified such as forged steel, cast steel, cast iron and rolled steel. The promising material will be selected by evaluating such as corrosion resistance, structural integrity and manufacturability. Cast iron has difficulty of welding, and the rolled steel has difficulty in the application to the overpack whose thickness is 190 mm [1]. Cast steel is seemed to be better than the above two candidates, however there are concerns about the presence of casting defects and the heterogeneity of metallographic structure and chemical composition, which may adversely affect corrosion resistance and structural integrity. On the other hand, forged steel has few defects, and has been used as a pressure vessel material such as a light water reactor, and has high reliability. Therefore, research and development of overpack so far has been carried out mainly on forged steel as the primary candidate material.

However, for reducing manufacturing cost, cast steel overpack may be effective as compared with forged steel overpack. This is because in the manufacturing of forged steel products, an ingot is produced from molten steel and then formed into a product shape by pressing or hammering, in contrast, cast steel products are manufactured with fewer steps as molten steel is cast in a mold near a product shape. Hence, we are now examining the applicability of

cast steel to overpack by investigating the technical concern as mentioned above.

First of all, the relationship between corrosion resistance and metallographic microstructure and chemical composition of cast steel which may distribute heterogeneously in the products has been investigated. Whether casting defects occurred in the corrosion allowance has also been confirmed. To reproduce realistic distributions of metallographic structure, chemical composition and casting defects, a full-scale cast steel overpack was fabricated. Then, microstructure observation, chemical composition analysis and corrosion tests using specimens taken from various positions in the cast steel overpack were carried out to evaluate the heterogeneity of corrosion resistance depending on the position of the overpack. Furthermore, it was confirmed by non-destructive testing whether casting defects occurred in the corrosion allowance, and the required additional corrosion allowance was considered if casting defects occurred.

2. Experimental method

2.1 Fabrication of full-scale cast steel overpack

Fig. 1 shows the dimensions of the manufactured overpack. The dimensions were based on the specification indicated by JNC [1], and the container part excluding the lid part was manufactured. The steel grade was the Japanese Industrial Standard, JIS G 5102 SCW 410. The reason for selection of this was that JIS G 5102 is cast steel with consideration for weldability and SCW 410 is a steel grade with low yield strength (the specification is 175 N/mm² or more) which is advantageous for resistance to

hydrogen-induced cracking (HIC) and weld cracking. As shown in Fig. 2, the overpack was cast larger than the designed dimensions in the inverted state and then machined. The heat treatment was conducted at 920 °C for 11 hours then furnace cooled as annealing for the purposes of removing internal stress and improving mechanical properties.

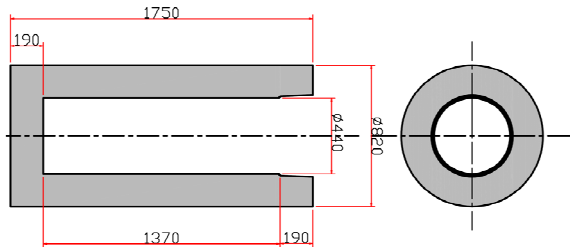


Fig. 1 Dimensions of fabricated overpack (mm)

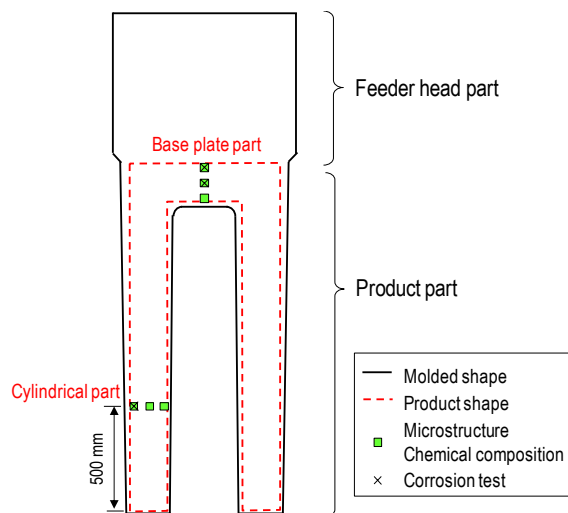


Fig. 2 Casting configuration and sampling positions for microstructural observation, chemical composition analysis and corrosion test

2.2 Non-destructive testing of casting defect

Magnetic particle testing (MT) and ultrasonic testing (UT) were conducted as non-destructive testing of casting defects. The test conditions are shown in Table 1.

Table 1 Test condition of MT and UT

	Magnetic particle testing (MT)	Ultrasonic testing (UT)
Testing area	Surface	Inside
Method	Yoke method	Vertical beam method
Procedure	JIS Z 2320	JIS Z 2344
Detection limit	≥ 1 mm	≥ 2 mm diameter

Table 2 Composition of the synthetic sea water (g/L)

NaCl	MgCl ₂	Na ₂ SO ₄	CaCl ₂	KCl	NaHCO ₃	KBr	H ₃ BO ₃	SrCl ₂	NaF
24.53	5.20	4.09	1.16	0.69	0.201	0.101	0.027	0.025	0.003

2.3 Microstructural examination and chemical composition analysis

As shown in Fig. 2, the specimens for microstructural observation (25 × 25 × 25 mm³) and the specimens for chemical composition analysis (25 × 25 × 25 mm³) were taken from six locations, that is, the outer surface, the center, and the inner surface of the base plate part and the cylindrical part. In the microstructure observation, after finishing the specimen to mirror, the surface etched in a nital solution was observed with an optical microscope. In the chemical composition analysis, the combustion-infrared absorption method was used for carbon (C) and sulphur (S), and the emission spectrometric analysis method was used for silicon (Si), manganese (Mn) and phosphorus (P).

2.4 Corrosion experiment

From six sampling positions where the microstructure observation and the chemical composition analysis were carried out, three points shown in Fig. 2 were selected as the sampling parts of the specimen for corrosion test (25 × 25 × 3 mm³). Two positions at the outer surface are selected because these positions are in the corrosion allowance layer, and one position at the center of the bottom plate part is selected because the bottom plate portion is the final solidified region so that the segregation and the peculiarity of metallographic structure may be occurred. The anodic / cathodic polarization tests were performed with a platinum sheet as the counter electrode and a standard calomel electrode (SCE) as the reference electrode. The polarization curves were measured at a scan rate of 20 mV/min. The exposure area of the specimens was 1 cm². The test solution was the synthetic sea water (pH 8.4) according to ASTM D1141 to simulate the disposal environment. Table 2 shows the composition of the synthetic sea water. Nitrogen gas was blown into the solution during the experiment and the experiment temperature was 80 °C. The number of specimens tested for each condition was two.

Two different corrosion conditions were assumed for the corrosion test. Just after the emplacement of overpack, the oxidizing environment can be expected. After the consumption of the residual oxygen by reducing substances in the back filled tunnels, the reducing conditions can be expected. The corrosion behavior for the former conditions was investigated with the anodic polarization test, while the latter one was done with the cathodic polarization test.

3. Results

3.1 Fabrication of full-scale cast steel overpack

Fig. 3 shows the photograph of the fabricated full-scale cast steel overpack. The chemical composition acquired by ladle analysis and the mechanical properties satisfied JIS G 5102.



Fig. 3 Photograph of the fabricated full-scale cast steel overpack with 1750 mm in length and 820 mm in diameter

3.2 Non-destructive testing of casting defect

Fig. 4 shows the distribution of casting defects obtained by MT performed as detection of surface defects. The type of casting defects was not a crack but a cavity. 82 defects were detected, almost all of them were detected at the bottom surface, and only one was detected at the side surface. Fig. 5 shows the number of casting defects as a function of distance from the periphery to the center of the bottom surface, with information of the size of casting defects. As can be seen from this figure, casting defects were distributed in the outer edge region of the overpack bottom surface with a peak at 20-30 mm from the periphery. The defect size was 1-5 mm, and there was the tendency to include larger defects as the distribution of the number of defects is close to the peak. On the other hand, the largest size of the casting defect found at the corner of bottom surface was 10 mm.

Fig. 6 shows the distribution of casting defects obtained by UT performed as detection of internal defects. 62 defects were detected and distributed in the lower half of the overpack. No casting defect was detected in the part of 440 mm radius from the center of the bottom plate part. In addition, Fig. 7 shows the distribution of the number of casting defects from the outer surface to the inner surface of the cylindrical body with information of the size of casting defects. Casting defects were distributed from the outer surface to the center of the cylindrical body thickness with a peak at the depth of 50-60 mm from the outer surface. The defect size was 2.0-3.6 mm, and there was the tendency to include larger defects as the distribution of the number of defects is close to the peak. Casting defects were found in the corrosion allowance layer whose thickness is 17 mm [2] from the outer surface.

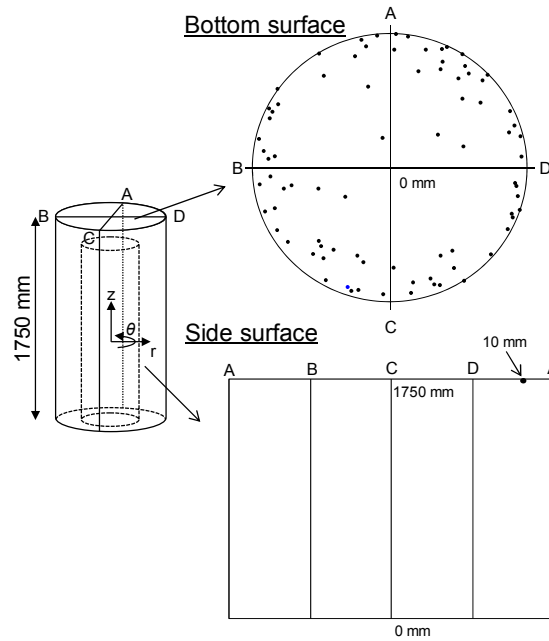


Fig. 4 Results of MT (surface defect testing)

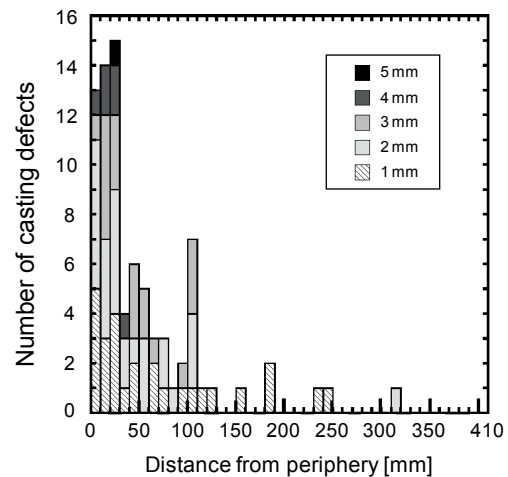


Fig. 5 Distribution of casting defects detected by MT from the periphery to the center of the bottom surface

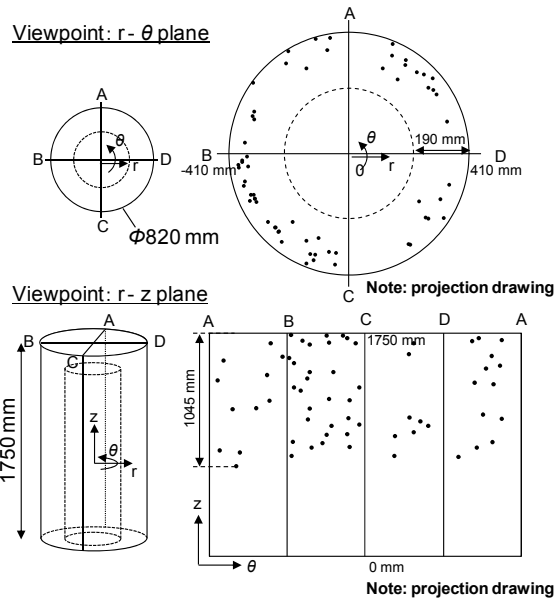


Fig. 6 Results of UT (inside defect testing)

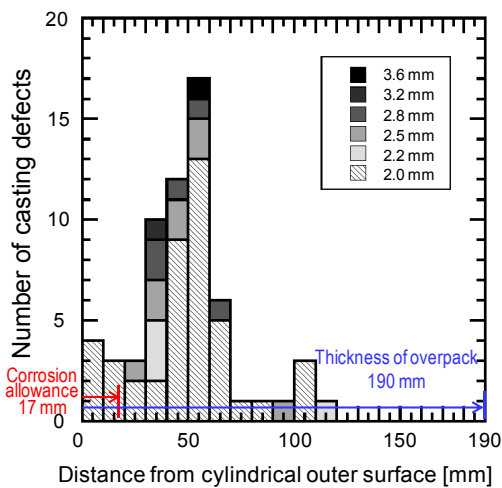


Fig. 7 Distribution of casting defects detected with UT from the outer surface to the inner surface of the cylindrical body

3.3 Microstructural observation and chemical composition analysis

Fig. 8 shows the microstructures at each position of specimen indicated in Fig. 2. The difference of microstructures was negligible between sampling positions.

Table 2 shows the analysis results of chemical composition for the specimens at each position indicated in Fig. 2. No significant difference was observed in the chemical compositions depending on sampling positions.

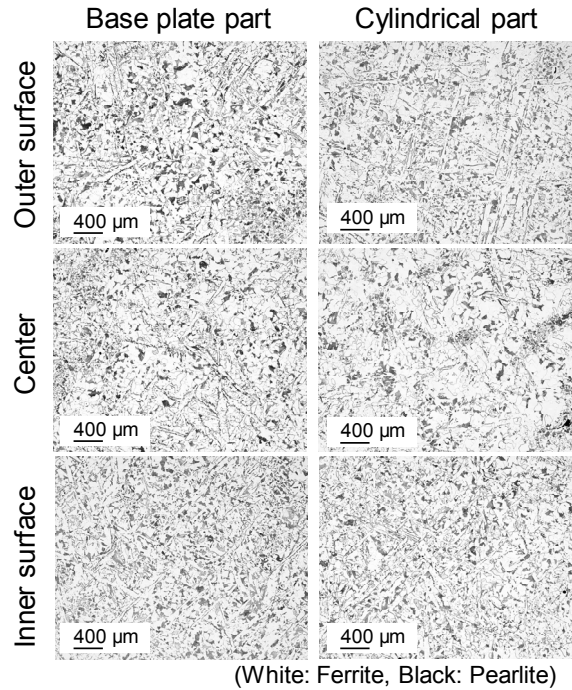


Fig. 8 Microstructures at six sampling positions

Table 2 Chemical compositions at each sampling position (wt-%)

		C	Si	Mn	P	S
Specification		<0.22	<0.80	<1.50	<0.040	<0.040
Ladle analysis		0.16	0.42	0.80	0.009	0.001
Base plate part	Outer surface	0.16	0.42	0.80	0.006	0.002
	Center	0.15	0.42	0.80	0.008	0.001
	Inner surface	0.19	0.43	0.83	0.010	0.006
Cylindrical part	Outer surface	0.17	0.44	0.84	0.011	0.002
	Center	0.15	0.42	0.80	0.008	0.001
	Inner surface	0.16	0.42	0.81	0.009	0.001

3.4 Corrosion experiment

Fig. 9 shows the anodic / cathodic polarization curve in synthetic sea water. There was no significant difference in any of the polarization curves between the different sampling positions.

Table 3 shows the corrosion current density obtained by extrapolating the tangent of the cathodic polarization curve in the Tafel region up to the corrosion potential. From this result, the behavior of hydrogen evolution reaction in synthetic sea water was similar between the sampling positions.

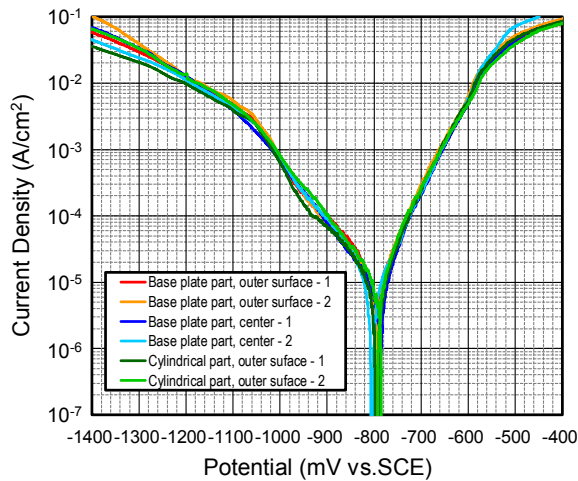


Fig. 9 Anodic / cathodic polarization curves in the synthetic sea water

Table 3 Corrosion current density of hydrogen evolution reaction in synthetic sea water

	Corrosion current density($\mu\text{A}/\text{cm}^2$)
Base plate part, outer surface-1	15
Base plate part, outer surface-2	12
Base plate part, center-1	8
Base plate part, center-2	15
Cylindrical part, outer surface-1	10
Cylindrical part, outer surface-2	10

4. Discussion

4.1 Effect of heterogeneity of microstructure and chemical composition on corrosion resistance

The heterogeneity of the microstructure and chemical composition of the cast steel was negligibly small. This may be a cause of homogeneous corrosion resistance. This is also indicative of the little possibility of macro cell corrosion induced by heterogeneity of microstructure and chemical composition.

4.2 Effect of casting defect on corrosion resistance

The large steel ingot has a characteristic segregation zone called inversed V-segregation zone, the inversed V-segregation zone appears from the outside to the center of the steel ingot close to the feeder head [3]. In this inversed V-segregation zone, micro shrinkage cavities are generated.

The size of casting defects found in this work was small. They distributed from the outer surface to the center of the cylindrical body close to the feeder head shown in Fig. 2. These observations suggested that the casting defects in this work were caused by inversed V-segregation peculiar to large cast steel products.

In order to reduce the occurrence of casting defects in the corrosion allowance, countermeasures are considered such as making the mold additionally larger than the product shape and thereby shifting the defect generation zone to the out of the product shape.

However, it is a trade-off with cost because the machining margin becomes larger, and it is considered difficult to completely eliminate casting defects, so that a method of providing the addition to corrosion allowance was examined as compensation for permitting the occurrence of casting defects in the corrosion allowance.

The examination of the additional corrosion allowance was carried out by using results of UT having information of three dimensional coordinates including thickness direction. As shown in Fig. 10, if casting defects exist in the corrosion allowance layer, it is assumed that the thickness corresponding to the size of the defects is not provided as corrosion allowance at the position where the defect exists. It is also necessary to consider the possibility that defects overlap in the thickness direction as shown in Fig. 10 (d). Therefore, in case the probability that defects overlap in the thickness direction was more than one out of 40,000 overpacks (i.e. more than 3×10^{-5}), the total dimension of overlapped defects was added to the corrosion allowance, otherwise, the dimension of one defect was added.

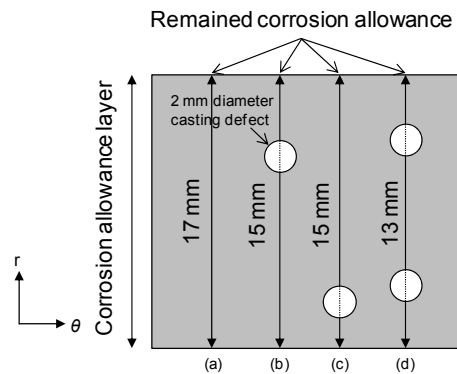


Fig. 10 Schematic diagram showing a state in which the required corrosion allowance is not ensured due to casting defects (Note: the axes corresponds to Fig. 6)

According to Fig. 6, casting defects existed in the region from the bottom surface to the height of 1045 mm. In addition, according to Fig. 7, the size of casting defects included in the region from the surface to 17 mm depth (which is the corrosion allowance) were all 2 mm. Therefore, it is supposed that 2 mm casting defects occur in random in this region. As shown in Fig. 11, the probability that two circles with a diameter of 2 mm overlap in the thickness direction is the probability that the center point of one circle is within 2 mm radius from the center point of the other circle. This probability is the square value of the value obtained by dividing the area of a circle with a radius of 2 mm by the area of the cylindrical outer surface from the bottom to the height of 1045 mm. This was calculated as 2×10^{-11} . In addition, since there were five casting defects in the

region from the surface to 17 mm depth, the combination that two out of the five casting defects overlap is ${}_5C_2 = 10$. Consequently, the probability that two out of the five casting defects of 2 mm diameter overlap is 2×10^{-10} . The probability of three or more overlapping is further reduced. Since it was much lower than the criterion of the probability (more than 3×10^{-5}), according to the result of this work, it was not necessary to consider the possibility of casting defects overlapping in the thickness direction, and it was considered appropriate to provide 2 mm as the additional corrosion allowance.

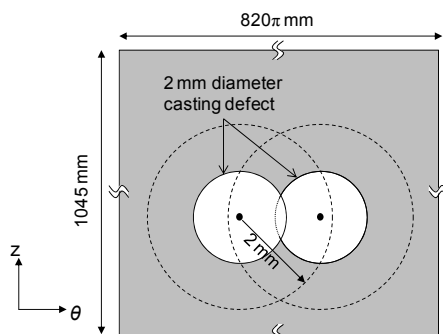


Fig. 11 Schematic diagram of overlapping of casting defects in the thickness direction (Note: the axes corresponds to Fig. 6)

Although the current reference thickness of the carbon steel overpack is set to 190 mm based on the evaluation by JNC [1], in the evaluation based on the latest knowledge, the required thickness of the overpack is 122 mm [3]. Thus, since the current specification of the carbon steel overpack has 68 mm as a margin, the additional corrosion allowance of 2 mm can be sufficiently ensured.

However, because the above evaluation was conducted within the current small amount of data, more detailed examination is necessary for accurate assessment of the additional corrosion allowance. Specifically, it is necessary to perform casting defects detection by X-ray computed tomography so as to detect casting defects below the detection limit of UT, to grasp the shape of casting defects and to obtain the position coordinates of casting defects more accurately. In addition, it is also considered necessary to observe the shape and the dimension of casting defects visually by cutting the cross section, and confirm the consistency with non-destructive testing. Furthermore, studies for confirming conditions of occurrence of casting defects and examinations based on a larger number of casting defect data are necessary.

5. Conclusion

By fabricating the cast steel overpack on a full-scale, the heterogeneities of the microstructure and chemical compositions were investigated and the

heterogeneity of corrosion resistance was examined by electrochemical corrosion test. These heterogeneities were negligible.

Non-destructive testing of the cast steel overpack was conducted, and the distribution and dimensions of casting defects were investigated. As a result, since the casting defect occurred in the corrosion allowance, a method of ensuring corrosion allowance by providing the additional thickness was examined. Consequently, the number of casting defects generated in the corrosion allowance layer was small and the dimensions were also small, so that the prospect of ensuring the corrosion allowance by providing an additional thickness of a few mm was indicated.

References

- [1] JNC (2000): H12: project to establish the scientific and technical basis for HLW disposal in Japan, Supporting Report 2, JNC TN1410 2000-003.
- [2] Ogawa, Y., Suzuki, S., Kubota, S., Deguchi, A. (2017): Re-evaluation of the required thickness of the carbon steel overpack for high-level radioactive waste disposal in Japan based on the latest scientific and engineering knowledge, *Corros Eng Sci Technol*, Vol.52, pp.204–209.
- [3] Ohno, A. (1973): *The Solidification of Metals*, Chijin Shokan Co.